Supplementary material for:

Ribosome provisioning activates a bistable switch coupled to fast exit from stationary phase

P. Remigi, G.C. Ferguson, S. De Monte and P.B. Rainey

This document contains:

- Supplementary Note
- Supplementary Figures 1-10
- Supplementary Tables 2-5

Supplementary Note:

Model for titration-based molecular switch

March 23, 2018

We model the intracellular dynamics by means of a set of ordinary differential equations describing the time evolution of the concentration of mRNA produced by a *gene with positive auto-regulation* (PFLU3655), and whose translation is post-transcriptionally modulated by the competition between ribosomes and a *regulator* (RsmA/E).

The model is inspired by Mukherji et al. Nature Genetics 2011, and its main features, derived from the experimental observations or hypothesized according to standard assumptions on molecular interactions, are illustrated in Fig. 1.

The time evolution of the system is described by three variables that quantify the concentrations of the three components of the mRNA pool: the concentration f of free mRNA, the concentration r of mRNA bound to ribosomes, and the concentration r^* of mRNA bound to the regulator. The level of fluorescence production, reporting the pathway involved in capsulation, is under the same positive regulation by the gene product as the gene itself. For simplicity, we will consider that the concentration of the protein coded by the gene is the same as for the mRNA undergoing translation, so that the feedback loop is modelled by the dependence on r on the production of new free mRNA. Similarly, r will measure the activation level of the fluorescent reporter/capsulation pathway.

The pools of free ribosomes ρ and of free regulator α interact post-transcriptionally with the free mRNA, competing for the same binding site, so that the regulator can sequester a fraction of mRNAs, analogously to what happens in other cases of molecular titration.

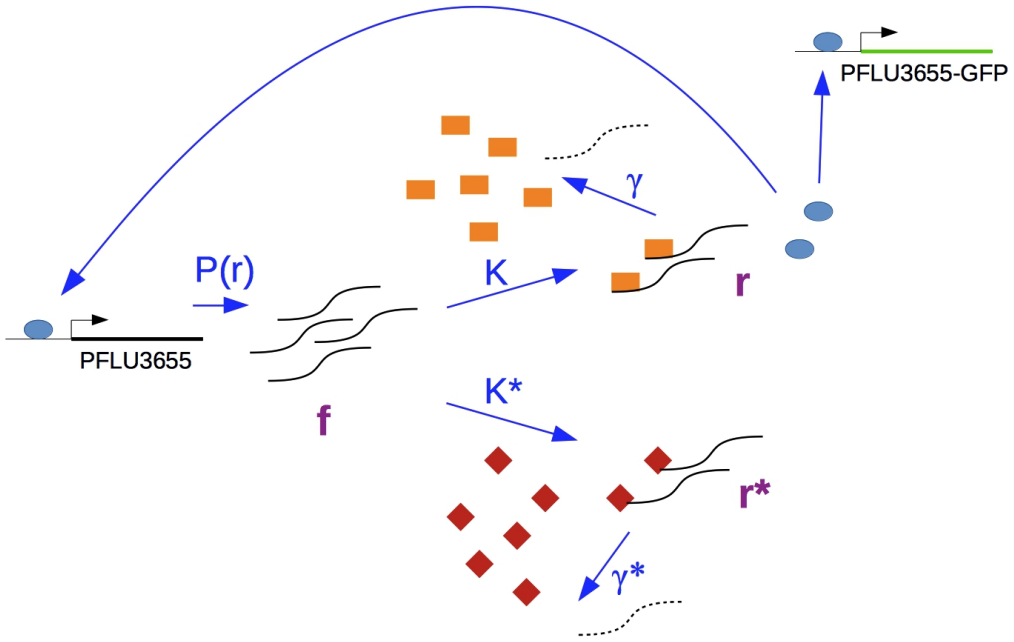

Figure S1: Schematic representation of the hypothesized regulatory pathways, involving competition between ribosomes (orange rectangles) and a regulator (red lozenges) for a target site on the mRNA, activation of the gene transcription by the gene product (blue ellipses), and the reporter construct. The model describes the dynamics of the free mRNA concentration f and of that of mRNA bound to either ribosomes (r) or to the regulator (r^*). The rates relative to the transition between these three classes and towards degradation are indicated in blue. The total pool of ribosomes and regulator proteins are assumed to be constant, so that these are either in free form or bound to the mRNA.

The equations for the time evolution of the three state variables read:

$$\frac{df}{dt} = P(r) - K\rho f - K^*\alpha f \quad (1)$$

$$\frac{dr}{dt} = K\rho f - \gamma r \quad (2)$$

$$\frac{dr^*}{dt} = K^*\alpha f - \gamma^* r^*, \quad (3)$$

where K and K^* are the kinetic constants for the binding of the mRNA to the ribosomes and the regulator molecules, respectively, and γ and γ^* are the decay constants of the two bound mRNA classes (upon which decay, ribosomes and regulators are recycled in the cellular pool). Under the assumption that the pools of ribosomes R and of regulators A change on a slower time scale with respect to the expression of the gene, and if we assume for simplicity that every bound mRNA interacts with a single ribosome/molecule of the regulator, then the pools of free ribosomes ρ and of free regulator α can be computed by subtraction as $\rho = R - r$ and $\alpha = A - r^*$.

The production term $P(r)$ accounts for the positive feedback loop, and is thus assumed to be a positive increasing function with r, saturating at a constant level. For illustration purpose, we will assume that the protein has a binary cooperative binding to the gene promoter, so that the production rate has the Hill's form:

$$P(r) = \frac{a\, r^2}{b + r^2}, \tag{4}$$

but qualitatively similar results hold as well for other functional forms, as discussed later.

Let us now find the equilibrium solutions for eqs. 1-3, which we will keep in a general form by expressing the production (source) and binding (sink) terms in the free mRNA's equation 1 as functions of the translated mRNA.

From eq. 2, we can obtain the equilibrium f as a function of r:

$$f(r) = \frac{\gamma r}{K(R - r)}. \tag{5}$$

By substituting in eq. 3, we obtain the equilibrium r^* as a function of r:

$$r^*(r) = \frac{A}{\frac{c}{g}\frac{R-r}{r} + 1}, \tag{6}$$

where $g = \gamma/\gamma^*$ and $c = K/K^*$.

The equilibrium condition for eq. 1 can now be expressed in terms of r. Let us define as:

$$\begin{aligned} T(r) &= K(R - r) f(r) - K^* \left[A - r^*(r)\right] f(r) = \\ &= \left[1 + \frac{A}{(g - c)\, r + cR}\right] \gamma\, r \end{aligned} \tag{7}$$

the term accounting for binding during post-transcriptional regulation. Since by definition $r < R$, the numerator in eq. 7 is always positive. $T(r)$ opposes

the increase in translation elicited, in absence of titration, by the positive feedback loop.

The equilibria of the system correspond to:

$$P(r) = T(r), \tag{8}$$

that is binding exactly balances production. When $P(r) > T(r)$, then the amount of free mRNA will increase in time, and vice-versa when $P(r) < T(r)$, so that the stability of the equilibria can be assessed by looking at the difference $P(r) - T(r)$ between source and sink terms.

In order to understand the qualitative behaviour of the different strains considered in the main text, we can study graphically the solutions to eq. 8 as the intersections of the two curves $P(r)$ and $T(r)$. For simplicity, we assume that the decay rates are constant and equal, thus $g = 1$. We study the number and position of the equilibria for a set of parameters that corresponds to the qualitative differences among the strains discussed in the main text: the WT, the 1B4 switcher mutant and two genetic constructs with increased production and decreased binding affinity of the regulator.

As illustrated in Fig. 2, the two curves always intersect in the origin (as long as the protein has no other sources of production than the self-regulated gene). Such trivial equilibrium corresponds to the 'OFF' state, where the gene is not expressed, and cells are not capsulated. If the term $T(r)$ is always larger than the production rate $P(r)$ (Fig. 2 A), then this equilibrium is stable. This case corresponds to the wild-type regulation in normal growth conditions, and occurs in a parameter range where the total concentration of regulator A is not too small relative to that of ribosomes R. Even in this situation it is nevertheless possible that, for large stochastic fluctuations, the system remains trapped for a certain time at high expression levels, due to the fact that the system slows down where the two curves approach, as illustrated by the proximity of the curve $P(r) - T(r)$ to the abscissae axis. This could correspond to the observation of rare, possibly transient, occurrences of capsulation in the SBW25 strain.

In switcher 1B4 strains and the wild-type strain in late stationary phase, where ribosome content is high with respect to the regulator, titration is only effective when the production, thus the protein concentration, is low. When the gene transcription exceeds a threshold (the middle, unstable equilibrium), instead, the production overcomes the post-transcriptional regulation, and

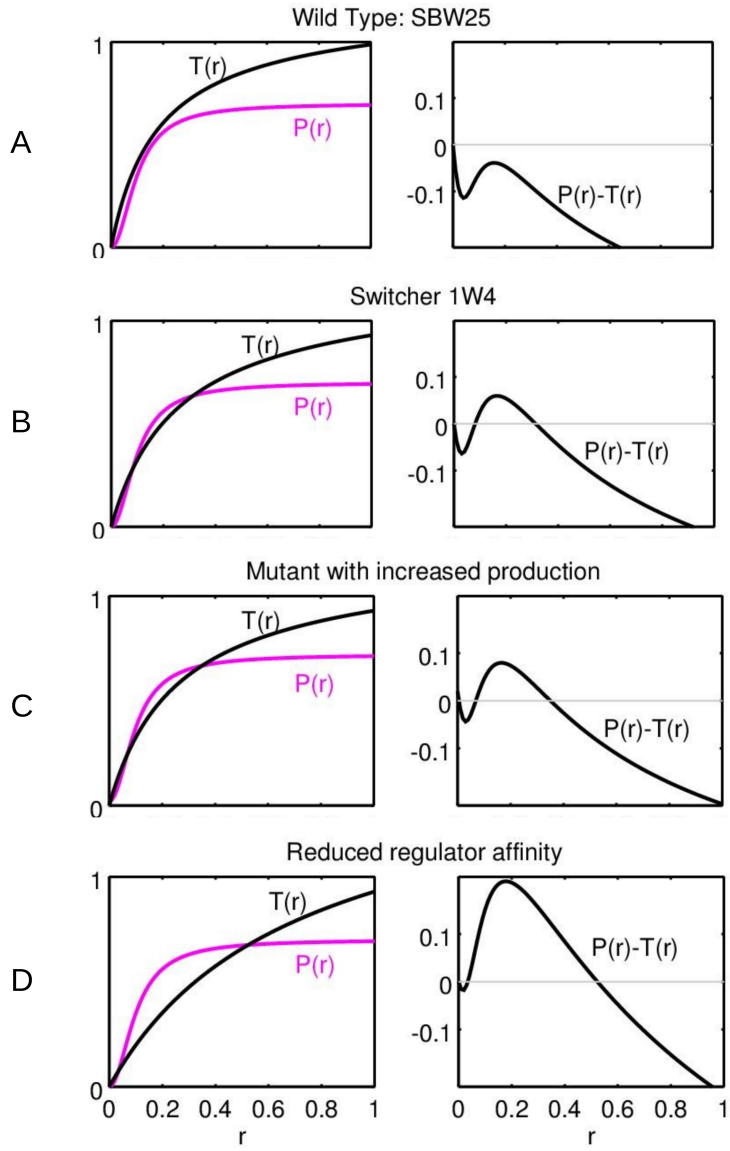

Figure S2: The intersection of the production curve $P(r)$ and of the curve $T(r)$ are the equilibrium points of eqs. 1-3. The figure illustrates the two qualitatively different scenarios that can occur: monostability of the 'OFF' state (A) and three different cases of bistability between 'OFF' and 'ON' states (B-D). Parameter values are: (A) $c = 0.2$, $R = 0.8$; (B) $c = 0.2$, $R = 1$; (C) $c = 0.2$, $R = 1$, but the production term is increased of $\delta = 0.05$; (D) $c = 0.3$, $R = 1$, and $g = 1$, and, in all cases, $\gamma = 0.02$, $A = 40$.

the amplification caused by the positive feedback loop displaces the system towards a new equilibrium. In such 'ON' equilibrium, the concentration of the transcript is no longer set by the regulator, but rather by other processes that impede the indefinite growth of protein production, such as for instance competition at the gene promoter binding site, which are recapitulated in the saturation of the production term.

If the production term had another functional form, the same type of scenario would occur, provided two conditions are satisfied:

- When the gene is expressed at very low levels, the production grows slower than the titration, so that most mRNA is sequestered by the regulator.
- Protein production saturates for high levels of translation, so that as to limit the autocatalitic effect of the positive feedback loop. For instance, this could be due to exhaustion of tRNAs.

If these conditions are met, then the system will be bistable whenever production outpaces titration for intermediate mRNA concentrations. The transition form a monostable to a bistable scenario corresponds to a (saddle-node) bifurcation occurring when the production curve is tangent to the regulation curve. This happens for parameters that satisfy the following equation, evaluated at the (parameter-dependent) equilibrium points r_E:

$$\frac{\partial P}{\partial r}(r_E) = \frac{\partial T}{\partial r}(r_E) \tag{9}$$

$$= \left\{ 1 + \frac{c\frac{A}{R}}{\left[(g-c)\,\frac{r}{R} + c\right]^2} \right\} \gamma. \tag{10}$$

Assuming that regulation of the gene is independent of post-transcriptional processes, thus keeps the same dependence on protein concentration when the interaction between mRNA and ribosomes/regulators is modified, the production term will be described by the same increasing function of r. Since the left-hand side of eq. 9 remains the same, hence, the transition to the bistability regime will occur for smaller r when the ratio A/R decreases. At the bifurcation point, the stable and unstable positive equilibria coincide, so that the threshold for the transition to the 'ON' state is smaller for higher levels of ribosomes relative to the regulator.

In the region where three equilibria are present, the position of the middle, unstable equilibrium defines the extension of the basins of attraction of the

two stable equilibria 'ON' and 'OFF'. If processes that are not included in this model, such as dynamical changes in other intracellular variables, or number fluctuations, cause stochastic variations in the number of proteins produced by the gene PFLU3655, it is reasonable to think that the relative extension of the basins of attraction quantifies the probability of finding a cell in one of either states, and that the position of the 'ON' equilibrium reflects the level of expression of the fluorescent marker.

Let us now consider if this qualitative model is consistent with the experimental observations relative to the genetic constructs in the 1B4 background studied in the main article, corresponding to Fig. 2 B in the model.

One first experiment consisted in duplicating the gene PFLU3655. Instead of being positively regulated by its own protein, the second copy is constitutively expressed, resulting in an effective increase of the transcription, independent on the protein concentration. We model this by adding to the production term a constant amount. If one substitutes $P(r)$ with $P(r) + \delta$, with $\delta > 1$, the basin of attraction of the 'OFF' equilibrium reduces, thus increasing the probability of switching to the 'ON' state (Fig. 2 C). At the same time, the production rate in the 'ON' equilibrium is slightly enhanced. This corresponds to an increase both of the proportion of cells in the 'ON' state and of their fluorescence, as observed experimentally.

In a second experiment, the binding affinity between the mRNA and the regulator was reduced, corresponding to an increase of the parameter c. This variation, illustrated in Fig. 2 D, leads as well to a steep increase of the probability of switching 'ON', as reported in Fig. 4c of the main text. Concomitantly, the production rate, hence fluorescence, increase, as also observed experimentally (Fig. 4b).

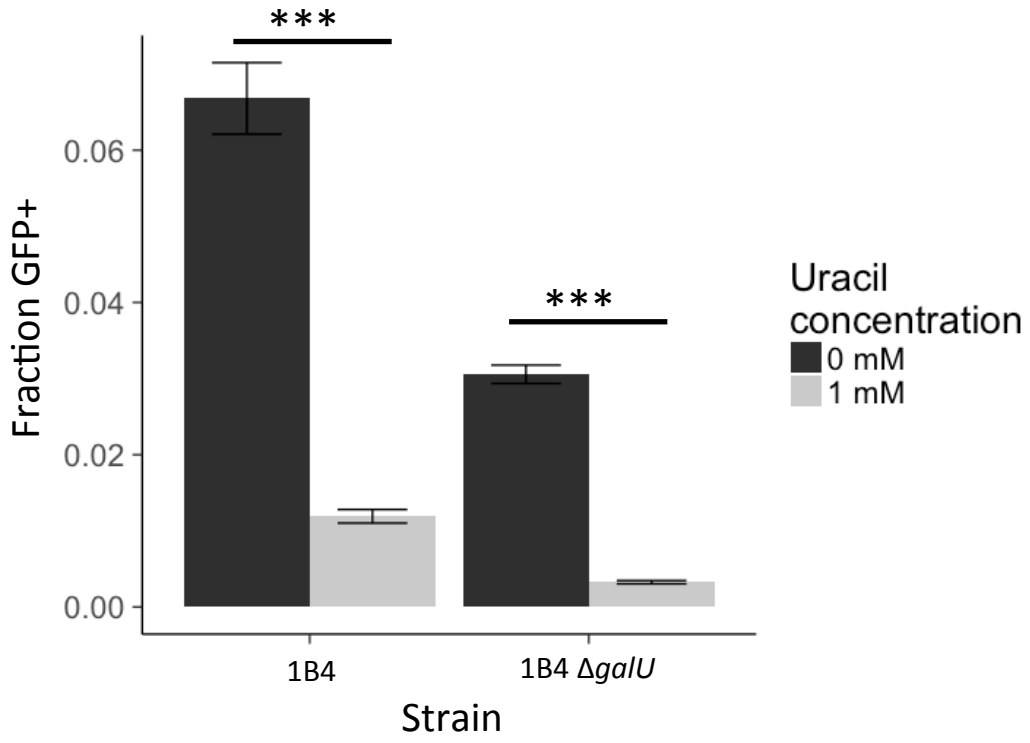

Supplementary Figure 1: Capsulation in the *galU* mutant

The Tn7-P*pflu3655*-GFP reporter was introduced in 1B4 and the *galU* transposon mutant[9]. Capsulation was measured by quantifying the proportion of GFP positive cells by flow cytometry at the onset of stationary phase. Means ± s.e.m. are shown, n = 12. Data are pooled from 2 independent experiments. *** $P < 0.001$, two-tailed *t*-test.

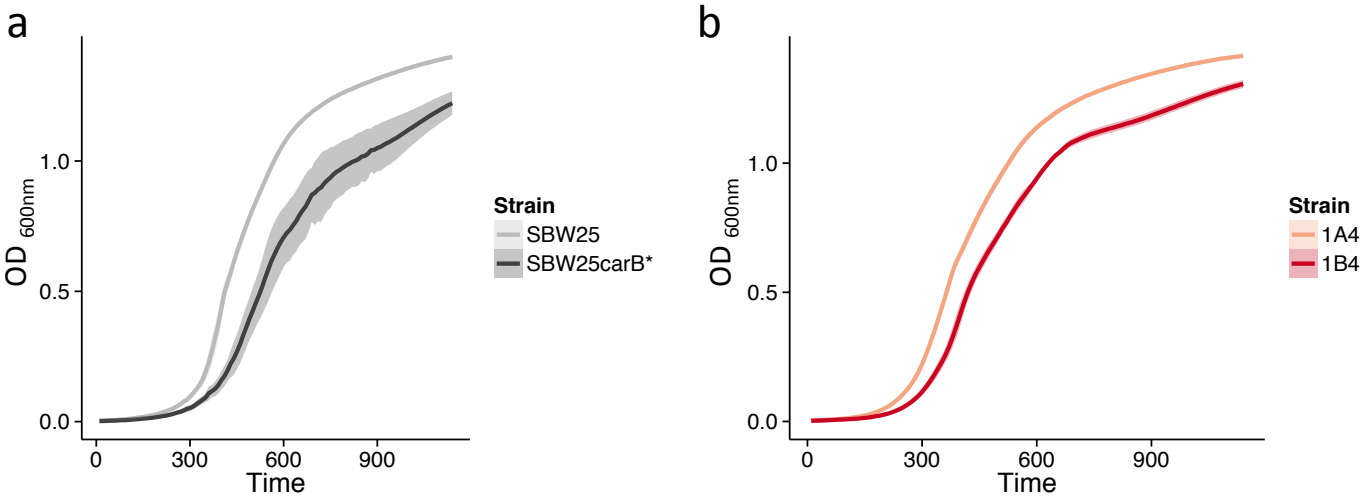

Supplementary Figure 2: Growth rate of *carB* mutants

Growth kinetics of SBW25 and SBW25 *carB* (**a**) or 1A4 and 1B4 (**b**) strains in KB medium. Lines and shading represent mean ± s.d., respectively, from 4 biological replicates.

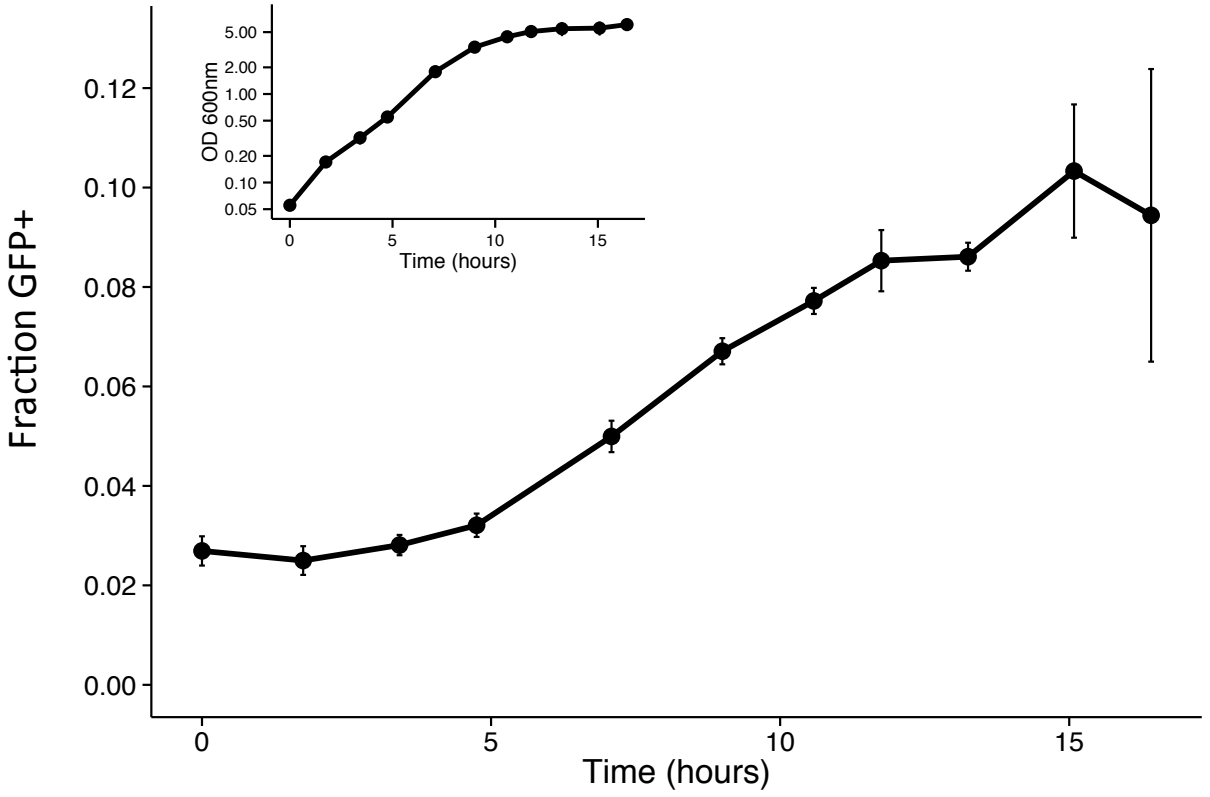

Supplementary Figure 3: Capsulation kinetics in 1B4

The Tn7-P*pflu3655*-GFP reporter was introduced in 1B4. OD600nm (inset) and size of GFP positive subpopulation (main panel) were monitored over >15h. Means ± s.d. are shown, n=3. Data are representative of 2 independent experiments.

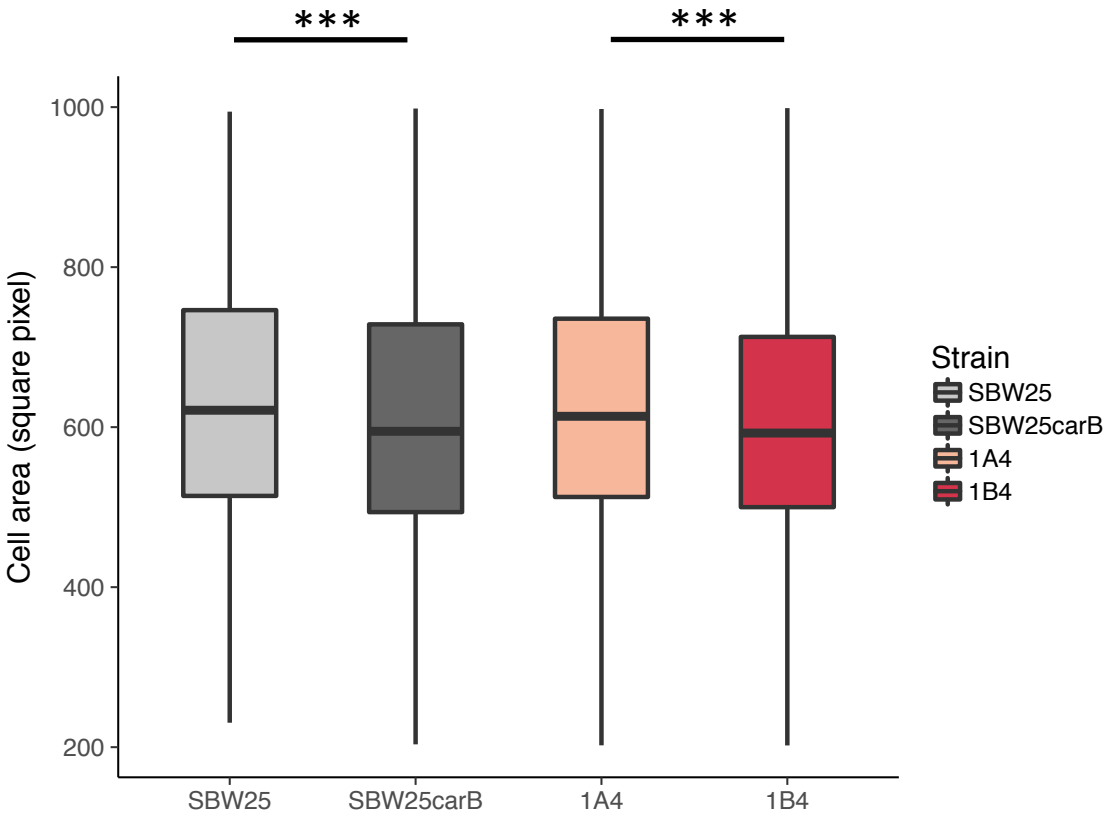

Supplementary Figure 4: The *carB mutation reduces cell size**

Boxplots represent the distribution of cell areas in exponentially growing cultures. n = 1760, 1535, 1420, 1399 for SBW25, SBW25 *carB**, 1A4 and 1B4, respectively. Data are pooled from 2 independent experiments. *** $P < 0.001$, Wilcoxon test.

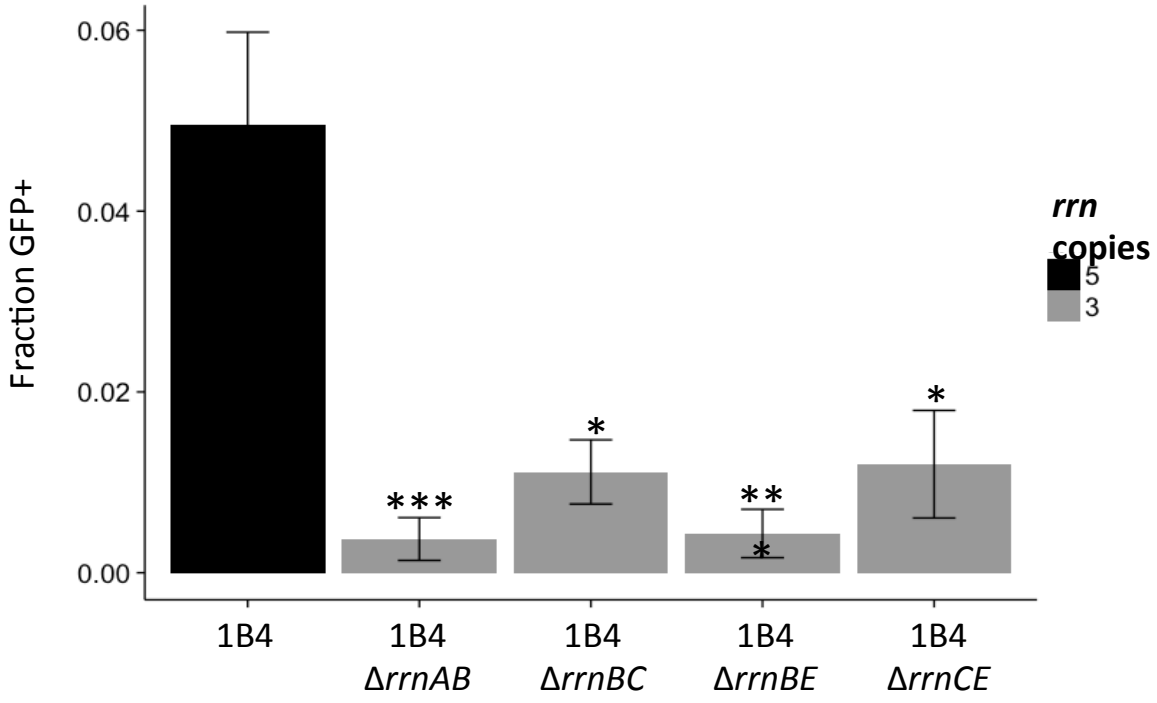

Supplementary Figure 5: Capsulation in double *rrn* mutants

Capsulation was measured by flow cytometry in 1B4 and its derived *rrn* double mutants at the onset of stationary phase (OD = 1-2). Means ± s.e.m. are shown. n = 9 (1B4 and 1B4 Δ*rrnCE*) or n = 18 (all other strains). Data are pooled from 3 independent experiments. * $P < 0.05$, *** $P < 0.001$, Kruskall-Wallis test with Dunn's post-hoc correction, comparison to 1B4.

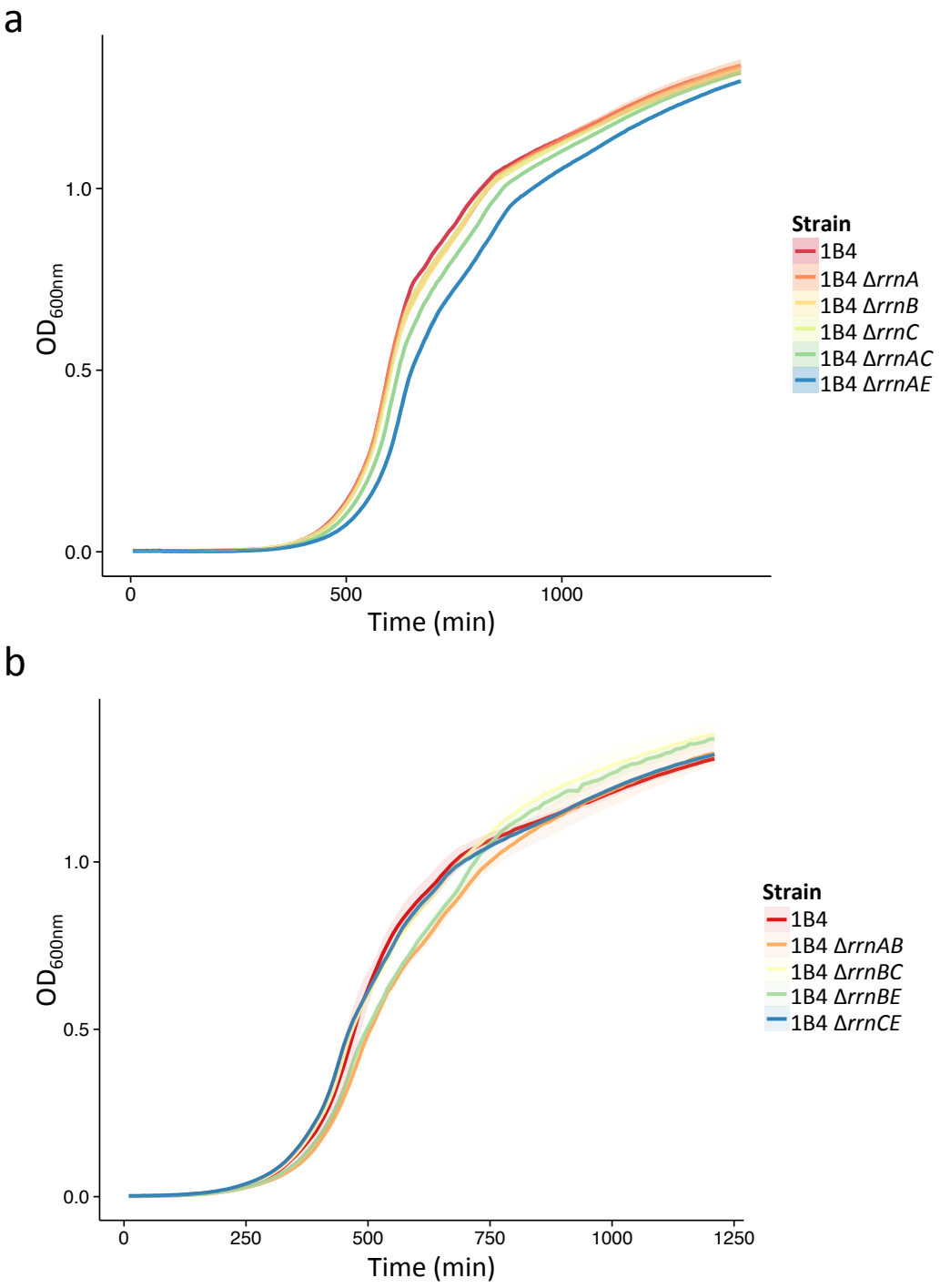

Supplementary Figure 6: Growth rate of *rrn* mutants

Growth kinetics of strain 1B4 and its derived double *rrn* mutants in KB medium. Lines and shading represent mean and s.d. from 4 biological replicates, respectively.

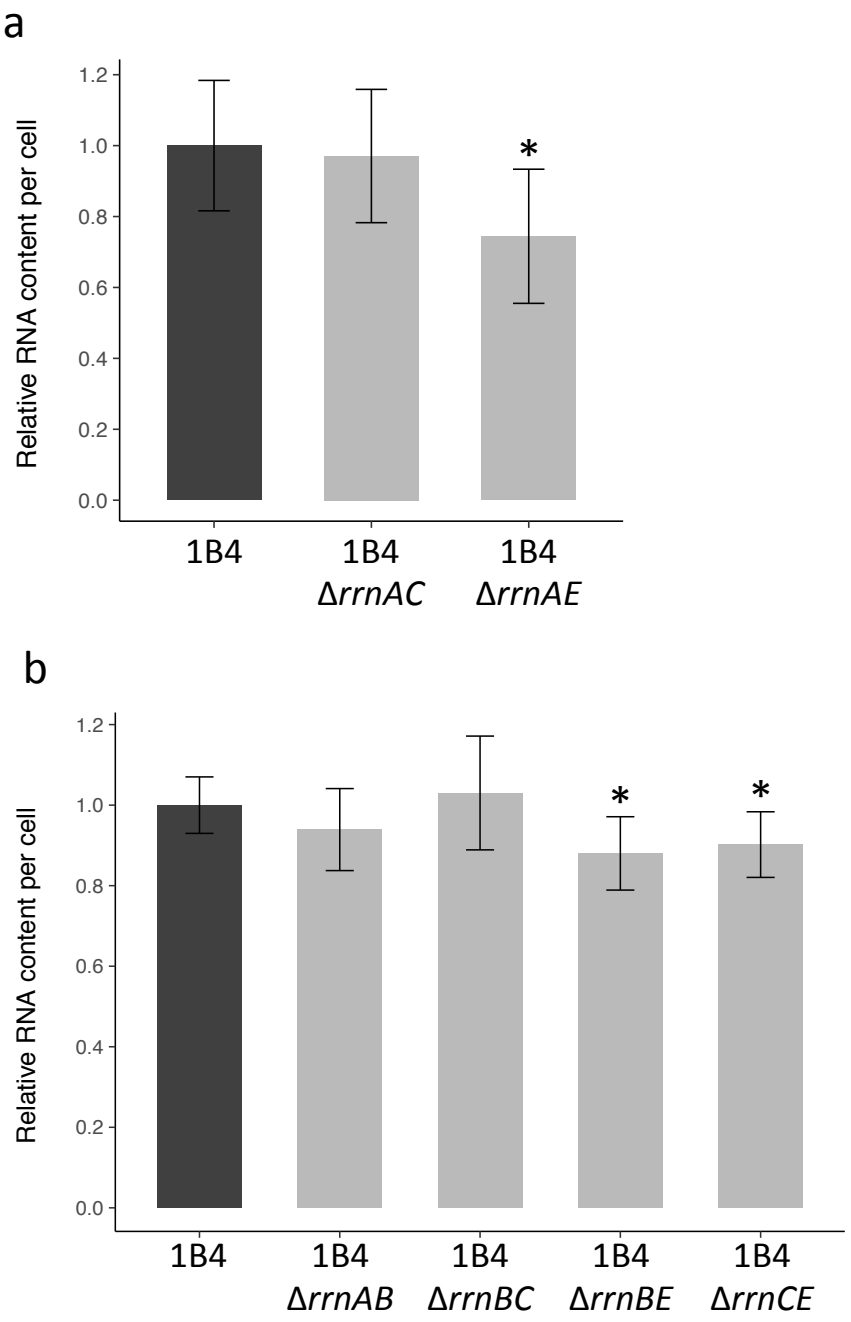

<u>Supplementary Figure 7: RNA quantification in *rrn* mutants</u>

Total RNA content in bacterial cells during exponential phase (OD = 0.5-0.6) normalized per cell count. Values were normalized to SBW25 or 1B4 controls within each experiment. Means ± s.d. are shown, n=6 (a) or n=8 (b). * $P <$ 0.05, two-tailed *t*-test compared to 1B4 values.

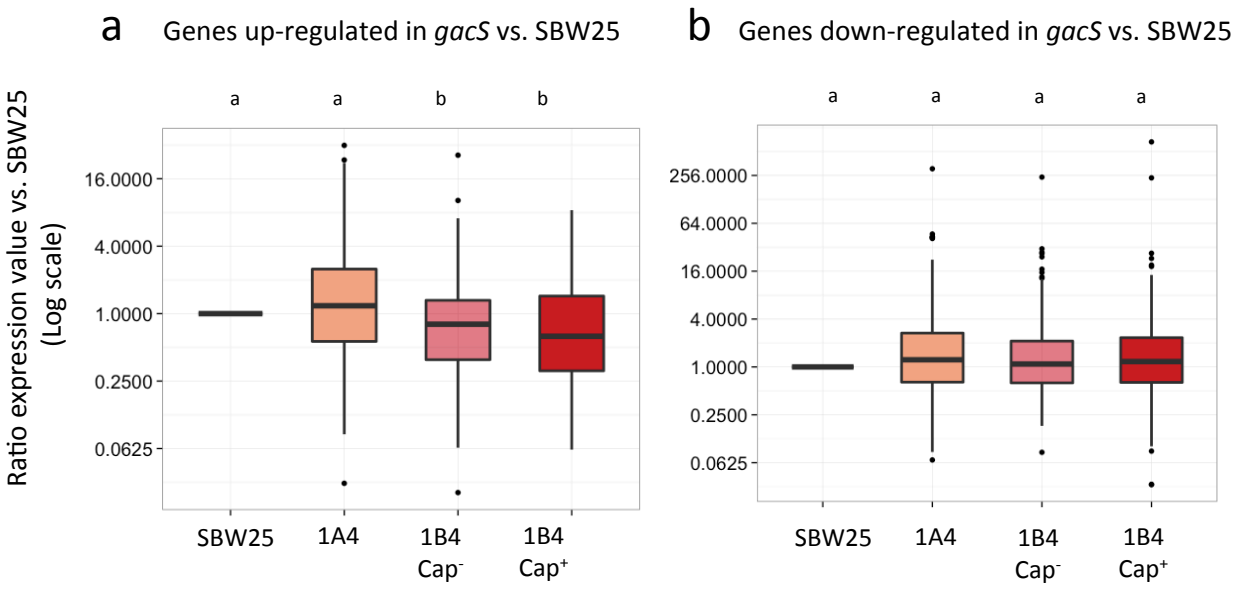

Supplementary Figure 8: Expression of *gacS*-regulated genes

Genes that are up-regulated (left) or down-regulated (right) more than 4 times in a *gacS* mutant compared to wild-type SBW25 were recovered from ref. 26. The distribution of induction or repression values (after normalisation by the base expression in SBW25) in the different RNA-seq datasets is shown for each set of genes. n = 125 (**a**) or n = 165 (**b**). Letter groups indicate statistical significance, $P < 0.05$, Kruskall-Wallis test with Dunn's post-hoc correction.

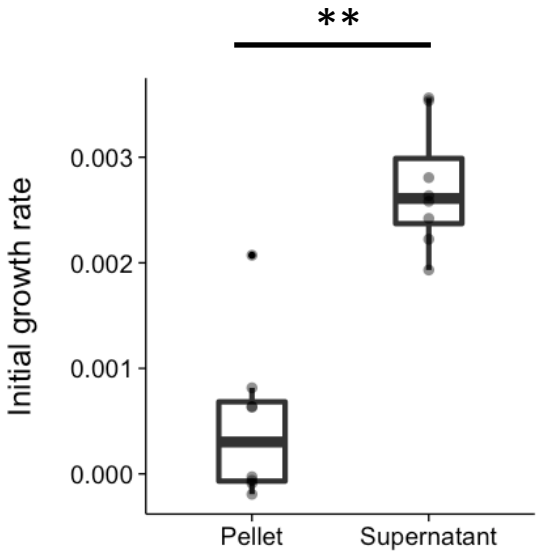

Supplementary Figure 9: Growth rate of SBW25 cultures enriched in Cap$^-$ or Cap$^+$ cells

Cells from 7 day-old colonies were resuspended in fresh KB and suspensions were enriched in Cap$^-$or Cap$^+$cells. Growth of these suspensions in 96-well plates was monitored for 2h. n = 8. Data are pooled from 2 independent experiments. ** *P* = 0.0078, Wilcoxon test.

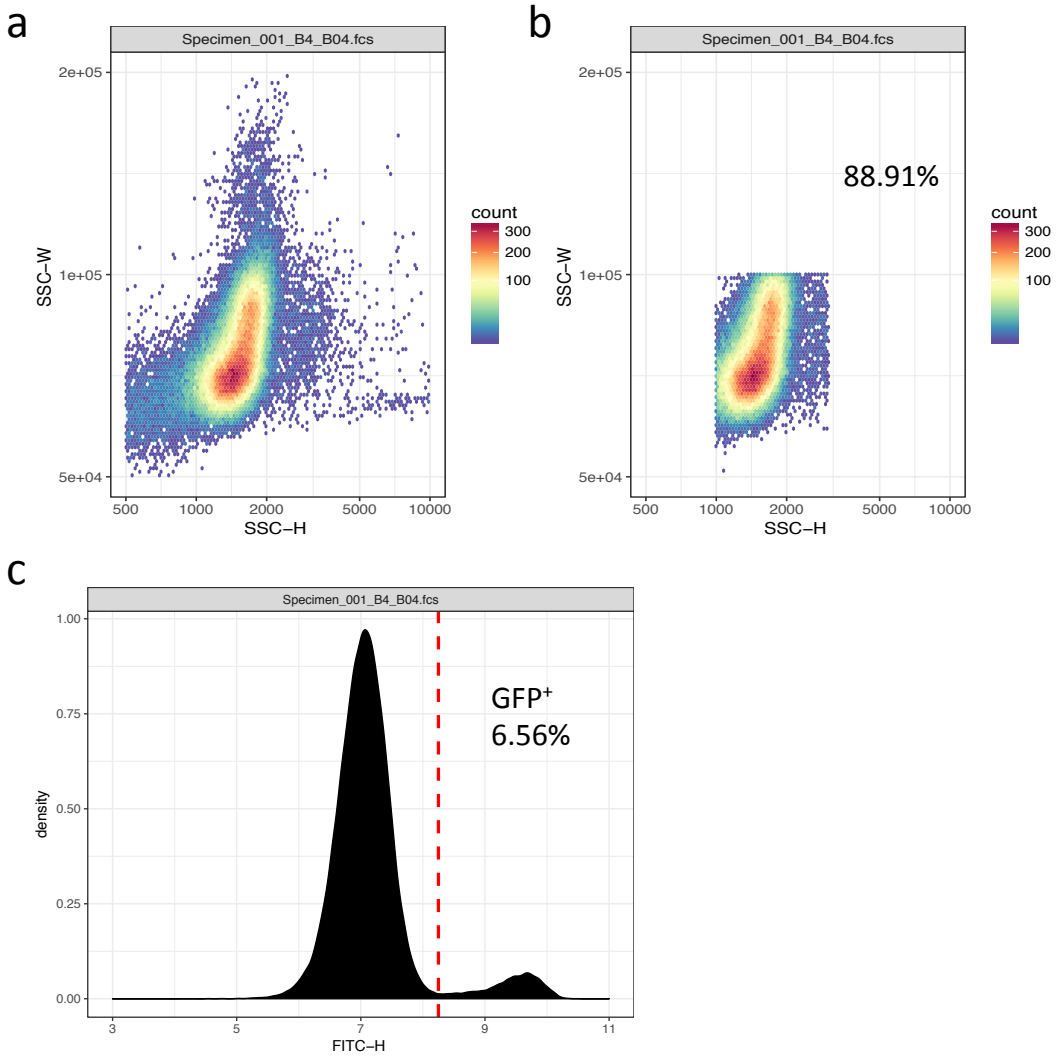

Supplementary Figure 10: Flow-cytometry gating strategy

(**a**) Between 20,000 and 100,000 events were recorded for each sample. (**b**) A first gating (function *rectangleGate* from the 'flowCore' package) was performed on SSC-H/SSC-W values, preserving typically 70-90% of the population. (**c**) For capsulation assays, GFP signal collected in the FITC-H channel was manually thresholded following bi-exponential transformation (function *biexponentialTransform* from the 'flowCore' package).

Strain	Reference
P. fluorescens	
SBW25	Zhang *et al.* 2006
SBW25 *lacZ*	Zhang & Rainey 2007
SBW25 *carB**	Beaumont *et al.* 2009
1A4	Beaumont *et al.* 2009
1B4	Beaumont *et al.* 2009
1B4 Tn5-*galU*	Gallie *et al.* 2015
1B4 Δ*rrnA*	This work
1B4 Δ*rrnB*	This work
1B4 Δ*rrnC*	This work
1B4 Δ*rrnE*	This work
1B4 Δ*rrnAC*	This work
1B4 Δ*rrnAE*	This work
1B4 Δ*rrnBC*	This work
1B4 Δ*rrnBE*	This work
1B4 Δ*rrnCE*	This work
1B4 Δ*pflu3655*	This work
1B4 ΔgacA	This work
1B4 Δ*rsmA1*	This work
1B4 Δ*rsmE*	This work
SBW25 P*pflu3655* G-8A	This work
SBW25 P*pflu3655* GG-7AC	This work
SBW25 P*pflu3655* A33T	This work
1B4 P*pflu3655* G-8A	This work
1B4 P*pflu3655* GG-7A	This work
1B4 P*pflu3655* A33T	This work

Supplementary Table 2: Bacterial strains used in this study

Name	Purpose	Description	Sequence
oPR156	Deletion *rrn* operons	*rrnB/C/E* overlap fwd	AAAACCCCATGAGAGGATCGAAACGTTAATAGAGC
oPR157		*rrnB/C/E* overlap rev	CGTTTCGATCCTCTCATGGGGTTTTGTTTTGGGCG
oPR158		*rrnB* up fwd	CAGTACTAGTCTTGTGGCCTGGATATGGGG
oPR159		*rrnB* down rev	CAGTACTAGTGGTACAAATCAGAATGCCTGCAT
oPR160		*rrnC* up fwd	CAGTACTAGTATATAGAATGTAGAGCGCCCAG
oPR161		*rrnC* down rev	CAGTACTAGTCCGTCCTACGTAACCGATCG
oPR164		*rrnE* down rev	CAGTACTAGTACCTGCTGATGGGGCGT
oPR165		*rrnE* up fwd	CAGTACTAGTGTCCATTGCTGATCCACCTCG
oPR166		*rrnA* up fwd	CAGTACTAGTAATTATCTGACGACAGGTGCCTC
oPR167		*rrnA* overlap rev	TGCCGCATCTGAGAGGATCGAAACGTTAATAGAGC
oPR168		*rrnA* overlap fwd	TTCGATCCTCTCAGATGCGGCAGTTGATAGATCC
oPR169		*rrnA* down rev	CAGTACTAGTCTACAGCTTGCTTGTACCAAGGA
oPR170	Site-directed mutagenesis of P*pflu3655*	*Ppflu3655* GG-7AC fwd	GCCTTGCATGCCGGAAAAGACAGTAGGTGATGCATTTTTC
oPR171		*Ppflu3655* GG-7AC rev	GAAAAATGCATCACCTACTGTCTTTTCCGGCATGCAAGGC
oPR174		*Ppflu3655* G-8A fwd	GCATCACCTACTCCTTTTTCCGGCATGCAAGGC
oPR175		*Ppflu3655* G-8A rev	GCCTTGCATGCCGGAAAAAGGAGTAGGTGATGC
oPR176		*Ppflu3655* A33T fwd	CTTTACGCATAGTCCGAGCAATAGCGAGGACGT
oPR177		P*pflu3655* A33T rev	ACGTCCTCGCTATTGCTCGGACTATGCGTAAAG
oPR37	Deletion *pflu3655*	*pflu3655* up fwd; SpeI	CAGTACTAGTCGTTTCTCGACAGCCTGGTG
oPR212		*pflu3655* overlap rev	CTCGCTATTCACCTACTCCCTTTTCCGGCATGC
oPR213		*pflu3655* overlap fwd	GAAAAGGGAGTAGGTGAATAGCGAGAAAATCCCCC
oPR214		*pflu3655* down rev; SpeI	TGACACTAGTATTGGGGGTGAAGTCGTGCA
oPR206	Complementation/over-expression *pflu3655*	*pflu3655* fwd; EcoRI	GATCGAATTCGTGATGCATTTTTCCAACGTCCT
oPR207		*pflu3655* rev; XhoI	GATCCTCGAGCTATTCACGATTCGACCGCTCC
oPR223	Reverse oligo to amplify *pflu3655* region (with oPR37)	*pflu3655* rev; SpeI	TGACACTAGTCTGCCTGACAATGTTGAAGTCA
oPR91	Deletion *rsmA1*	*rsmA1* up fwd; SpeI	TCAGACTAGTTCAATCAGTCAATTCATGATTGGTAAA
oPR92		*rsmA1* overlap rev	GTGAGGAGAAAGGTATGGAACCAAGCCTTTAATTTTTATC GTT
oPR93		*rsmA1* overlap fwd	AATTAAAGGCTTGGTTCCATACCTTTCTCCTCACGCAT
oPR94		*rsmA1* dwn rev; SpeI	TCAGACTAGTCAGCCTCGGTTCAAAGGTGT
oPR97	Deletion *rsmE*	*rsmE* up fwd; SpeI	TCAGACTAGTAGACCGTGGCGTGTGTGAT
oPR98		*rsmE* overlap rev	GCTACTGAGGGGGCTATGTTTCAGACAGGGCAGGT
oPR99		*rsmE* overlap fwd	CCCTGTCTGAAACATAGCCCCCTCAGTAGCCAG
oPR100		*rsmE* down rev; SpeI	TCAGACTAGTCGCAATTACCGGAATCGTGC
oPR148	P*rrnB*-GFP reporter	P*rrnB* up fwd; SpeI	CAGTACTAGTTATGCATCTATAGGTGCGCTGC
oPR151		P*rrnB*-GFP overlap rev	TCCTCTTTAATCTTCAGTTCAAACATCTTTGGGTT
oPR152		P*rrnB*-GFP overlap fwd	TGAACTGAAGATTAAAGAGGAGAAATTAAGCATGCG
FluomarkerP2		*gfpmut3*-T0 down rev	AATCTAGAGGATTCTCACCAATAAAAAACG

Supplementary Table 3: Oligonucleotides used in this study

Plasmid	Description	Reference or source
pRK2013	Helper plasmid, Tra^{+} Kan^{R}	Ditta *et al.* 1980
pUX-BF13	Helper plasmid for transposition of the Tn7 element, Amp^{R}	Bao *et al.* 1991
pUC18R6K-mini-Tn7T-Gm	A Tn7-based integration vector, Gen^{R}	Choi *et al.* 2005
pUC18R6K-mini-Tn7T-Gm-P*pflu3655*-GFP	Cloning of the promoter of *pflu3655* fused to *gfpmut3* into pUC18R6K-mini-Tn7T-Gm, Gen^{R}	Gallie *et al.* 2015
pUC18R6K-mini-Tn7T-Gm-P*pflu3655*-GFP G-8A	Introduction of the G-8A mutation by site directed mutagenesis into pUC18R6K-mini-Tn7T-GmPpflu3655-GFP, Gen^{R}	This work
pUC18R6K-mini-Tn7T-Gm-P*pflu3655*-GFP GG-7AC	Introduction of the GG-7AC mutation by site directed mutagenesis into pUC18R6K-mini-Tn7T-GmPpflu3655-GFP, Gen^{R}	This work
pUC18R6K-mini-Tn7T-Gm-P*pflu3655*-GFP A33T	Introduction of the A33T mutation by site directed mutagenesis into pUC18R6K-mini-Tn7T-GmPpflu3655-GFP, Gen^{R}	This work
pUC18R6K-miniTn7-P*rrnB*-GFP	Cloning of the promoter of *rrnB* fused to *gfpmut3* into pUC18R6K-mini-Tn7T-Gm, Gen^{R}	This work
pME6032	Shuttle vector for gene expression in Pseudomonas, Tet^{R}	Heeb *et al.* 2002
pME6032-*pflu3655*	pME6032 containing the *pflu3655* gene, Tet^{R}	This work
pUIC3	Integration vector with promoterless '*lacZ*, Mob^{+} Tet^{R}	Rainey 1999
pUIC3-Δ*rrnA*	Construct for *rrnA* deletion cloned into pUIC3, Tet^{R}	This work
pUIC3-Δ*rrnB*	Construct for *rrnB* deletion cloned into pUIC3, Tet^{R}	This work
pUIC3-Δ*rrnC*	Construct for *rrnC* deletion cloned into pUIC3, Tet^{R}	This work
pUIC3-Δ*rrnE*	Construct for *rrnE* deletion cloned into pUIC3, Tet^{R}	This work
pUIC3-Δ*pflu3655*	Construct for *pflu3655* deletion cloned into pUIC3, Tet^{R}	This work
pUIC3-P*pflu3655* G-8A	G-8A site-directed mutagenesis in P*pflu3655* for re-introduction into SBW25 genome, Tet^{R}	This work
pUIC3-P*pflu3655* GG-7AC	GG-7AC site-directed mutagenesis in P*pflu3655* for re-introduction into SBW25 genome, Tet^{R}	This work
pUIC3-P*pflu3655 A33T*	A33T site-directed mutagenesis in P*pflu3655* for re-introduction into SBW25 genome, Tet^{R}	This work
pUIC3-Δ*gacA*	Construct for *gacA* deletion cloned into pUIC3, Tet^{R}	XX. Zhang
pUIC3-Δ*rsmA1*	Construct for *rsmA1* deletion cloned into pUIC3, Tet^{R}	This work
pUIC3-Δ*rsmE*	Construct for *rsmE* deletion cloned into pUIC3, Tet^{R}	This work

Supplementary Table 4: Plasmids used in this study

Figure 1a

P-values:	1A4	1B4 Cap-	1B4 Cap+
1B4 Cap-	0.0004		
1B4 Cap+	< 0.0001	0.0082	
SBW25	0.4447	0.0005	< 0.0001

Figure 1c

	SBW25 vs. SBW25 carB	1A4 vs. 1B4
t	-4.005	-4.563
df	5.2935	8.5243
P-value	0.0009147	0.001565
95% CI	-1.089;-0.246	-0.906; -0.302

Figure 2a

	n	P value against 1B4
1B4	11	
rrnA	11	0.1804
rrnB	8	0.4616
rrnC	11	0.601
rrnAC	11	0.0164
rrnAE	11	< 0.0001

Figure 2b

	n	P value against 1B4
1B4	12	
gacA	15	0.008
rsmA	9	0.0014
rsmE	9	0.0471

Figure 4c

	n	P value against 1B4
1B4	9	
G-8A	9	0.0418
A33T	9	0.1522
GG-7AC	9	0.0009

Figure 4d

	n	P value against 1B4
SBW25	7	
G-8A	7	0.0035
A33T	7	0.9539
GG-7AC	7	0.9482

Figure 5b

t	-6.9625
df	186.6
P-value	5.53E-11
95% CI	-0.001438; -000803

Figure 6d

	T2	T4
t	2.4842	6.0219
df	11	11
P-value	3.03E-02	8.65E-05
95% CI	0.0184; 0.3039	0.433;0.932

RT-qPCR SBW25

	T2
t	4.3224
df	4
P-value	1.24E-02
95% CI	0.2421; 1.112

Figure S1

	1B4	1B4 galU
t	11.491	22.305
df	11.797	11.376
P-value	9.25E-08	5.68E-11
95% CI	0.0445; 0.0653	0.0246; 0.0299

Figure S4

	SBW25 vs. SBW25 carB	1A4 vs. 1B4
P value	0.0002099	0.0004005

Figure S5

	n	P value against 1B4
1B4	9	
rrnAB	18	< 0.001
rrnBC	18	0.0418
rrnBE	18	< 0.001
rrnCE	9	0.0462

Figure S7a

	rrnAC	rrnAE
t	0.2329	2.5317
df	9.8783	9.9925
P-value	0.8206	0.0298
95% CI	-0.298; 0.368	0.047; 0.74

Figure S7b

	rrnAB	rrnBC	rrnBE	rrnCE
t	0.34085	0.42404	5.4484	3.8465
df	12.792	10.211	13.335	13.958
P-value	0.7388	0.6803	0.0001019	0.001789
95% CI	-0.086; 0.119	-0.113; 0.167	0.147; 0.341	0.069; 0.243

Figure S8a

	1A4	1B4 Cap-	1B4 Cap+
1B4 Cap-	0.028		
1B4 Cap+	0.0004	0.5174	
SBW25	0.8842	0.0036	0.004

Figure S8b

	1A4	1B4 Cap-	1B4 Cap+
1B4 Cap-	0.7544		
1B4 Cap+	0.8	0.6858	
SBW25	0.2556	0.318	0.1884

Supplementary Table 5: List of all *P* values